## Title

Assessment of the performance of several novel approaches to improve physical properties of guar gum based biopolymer films



## Authors

Kirtil, Emrah
Aydogdu, Ayca
Svitova, Tatyana
et al.

## Publication Date

2021-09-01

## DOI

10.1016/j.fpsl.2021.100687

Peer reviewed

Food Packaging and Shelf Life 29 (2021) 100687

Contents lists available at ScienceDirect

Food Packaging and Shelf Life

journal homepage: www.elsevier.com/locate/fpsl

# Assessment of the performance of several novel approaches to improve physical properties of guar gum based biopolymer films

Emrah Kirtil [a,b,*], Ayca Aydogdu [a,c], Tatyana Svitova [a], Clayton J. Radke [a]

[a] Chemical and Biomolecular Engineering Department, University of California Berkeley, 101E Gilman, Berkeley, CA 94720-1462, USA
[b] Food Engineering Department, Yeditepe University, 34755 Kayisdagi, Istanbul, Turkey
[c] Department of Food Technology, Canakkale 18 Mart University, 17020, Canakkale, Turkey

ARTICLE INFO

*Keywords:*
Guar gum
Biodegradable film
Halloysite nanotube
Antimicrobial film
Emulsion film
Crosslinking

ABSTRACT

Biopolymer-based films are natural, renewable, nontoxic and biodegradable alternatives to plastic packaging. Despite years of ongoing research, biopolymer films still lag much behind plastic films in mechanical and barrier properties. In this study, guar gum (GG) based films were prepared to evaluate the potential of some novel applications in enhancing films physical properties. For this purpose, GG and glycerol based films were prepared with varying amounts of orange peel oil (1%, 2% v/v), and/or reinforced with halloysite nanotubes (HNT), and crosslinked with sodium trimetaphosphate (STMP). Oil incorporation, despite weakening films' mechanical strength, increased film hydrophobicity and enhanced its water barrier properties. Crosslinking, decreased films' relatively high solubility while also improving other film properties. Orange peel oil preserved its antimicrobial activity and HNT stabilized GG films provided controlled release of volatile essential oil. Findings indicated the possibility of improving physical properties of GG films with the methods employed.

## 1. Introduction

Packaging constitutes 40 % by weight of our solid wastes (Benbettaïeb, Gay, Karbowiak, & Debeaufort, 2016). Growing health concerns and increasing awareness on environmental "footprint" of our products creates a necessity for replacement of synthetic packaging materials. Biodegradable films made from environmentally friendly materials are good alternatives to plastic packaging (Hoque, Benjakul, & Prodpran, 2010). Biopolymer-based films, in particular, when used as food packaging materials, bypass the health concerns associated with food-package contact and possible harmful monomer migration especially in high pHs and/or temperatures (Guerreiro, de Oliveira, Melo, de Oliveira Lima, & Catharino, 2018).

Biopolymer-based films are natural, renewable, nontoxic and biodegradable and can cover the food providing a mild protection against mechanical stress while also acting as a barrier against moisture, $O_2$, aroma or lipid migration between different foods in a single package or between the food and the headspace of conventional packaging (Benbettaïeb et al., 2016; Gomaa, Hifney, Fawzy, & Abdel-gawad, 2018). Despite the advantages of biodegradable packaging materials, they still only represent less than 10 % of all commercial packaging in use (Xiao, Wang, Yang, & Gauthier, 2012). Biopolymer films made out of proteins, carbohydrates or combinations of these are even less commercially available. Despite years of ongoing research, biopolymer films are still lagging much behind plastic films in terms of mechanical and water barrier properties (Yin et al., 2015).

The inherent hydrophilicity of proteins and carbohydrates that form the basis of these biopolymeric films, gives it high water solubility and poor water barrier properties (Azeredo et al., 2017; Ke et al., 2019). This greatly limits their application. To overcome this limitation, lipids could be incorporated into the films. Emulsion films prepared by incorporation of lipids into carbohydrate/protein-polymer matrix was demonstrated to increase films' water barrier properties. The homogeneous distribution of lipids plays a key role in emulsion films properties (Galus, 2018). By inclusion of essential oils that show antimicrobial and antioxidant properties, supplementary functions could be assigned to these packages. Essential oils, having low-water solubility, are rather difficult to incorporate into aqueous-based foods. Additionally, their application in food systems is limited by flavor considerations as essential oils have volatile flavor components which give them dominant flavors (Acevedo-Fani, Salvia-Trujillo, Rojas-Graü, & Martín-Belloso, 2015). Dispersion of essential oils into food packaging instead of foods themselves

* Corresponding author at: Food Engineering Department, Yeditepe University, 34755 Kayisdagi, Istanbul, Turkey.
*E-mail addresses:* emrah.kirtil@yeditepe.edu.tr (E. Kirtil), ayca.aydogdu88@gmail.com (A. Aydogdu), svitova@berkeley.edu (T. Svitova), radke@berkeley.edu (C.J. Radke).

https://doi.org/10.1016/j.fpsl.2021.100687
Received 24 December 2019; Received in revised form 5 May 2021; Accepted 11 May 2021
Available online 8 June 2021

overcomes these limitations. Orange peel oil, which is an essential oil, is extracted from citrus/orange peels and is rich in monoterpenic hydrocarbons, with the main component being *d*-limonene (up to 97.3 g in 100 g orange peel oil) that has been shown to possess antimicrobial properties (Aboagye, Banadda, Kiggundu, & Kabenge, 2017; Kotsampasi et al., 2018).

Emulsions are thermodynamically unstable systems, thus are prone to destabilization. It is possible to form meta-stable emulsions by utilization of surface adsorbing molecules. In addition to surfactants, emulsions could also be stabilized by solid particles that adsorb on the oil-water interface. These dispersions, called Pickering emulsions, are prepared by irreversible adsorption of solid particles at the oil-water interface and build rigid physical barriers against coalescence (Yin et al., 2015). This type of stabilization mechanism may prove advantageous compared to surfactant-based stabilization and proves especially useful in foamed emulsions (Rutkevičius, Allred, Velev, & Velikov, 2018). Halloysite nanotubes (HNT) are materials composed of double layered aluminosilicate minerals with a predominantly hollow tubular structure in submicron range (Meira, Zehetmeyer, Werner, & Brandelli, 2017) and can function as solid emulsion stabilizer particles. HNT is a subgroup of kaolin clay and is generally recognized as safe (GRAS) for use in food packaging materials by U.S. Food and Drug Administration (FDA) owing to its biocompatibility, non-toxicity and environmental friendliness (Lee, Kim, & Park, 2018). When nanoclay minerals incorporated and exfoliated in the polymer matrix, they form tortuous pathways for vapor and gas molecules to pass through, which slows down the rate of diffusion (Lee et al., 2018). This phenomenon was observed as increased barrier properties for films reinforced with nanofillers. Additionally, nanofillers also provided films with better mechanical strength (Meira et al., 2017). Thus, the choice of HNTs as emulsion stabilizers could also overcome some of the weaknesses of biopolymer films.

Guar gum (GG) is a natural, nonionic, hydrophilic carbohydrate polymer, that is widely used in the food industry as a thickener and stabilizer (Moreira et al., 2012). It is composed of a long linear β-(1.4)-mannose backbone to which α-(1.6)-linked galactose residues are attached. The high number of hydroxyl groups in its structure grants it a very high water solubility (Variyar et al., 2015). GG was shown to form homogenous edible films that are almost completely water soluble (Borges, Banegas, Porto & Zornio, 2013). Water solubility is another important parameter that, depending on the film's intended use, could either be desirable or undesirable. However, there is no denying that high water solubility narrows down films application to only foods that are low in moisture content. Phosphate crosslinking of GG has been shown to decrease its solubility as well as assigning films made out of GG enhanced physical properties (Borges et al., 2013; Yıldırım-Yalçın, Şeker, & Sadıkoğlu, 2019). sodium trimetaphosphate (STMP) is a safe, non-toxic, FDA approved cross-linking agent commonly used for cross-linking starch in the food industry (Gliko-Kabir, Penhasi, & Rubinstein, 1999; Huang et al., 2019). At basic pHs, a complex of di-polymer phosphate ester is formed from GG and STMP. The hydroxyl groups in GG molecules could attach to the phosphate through phosphorylation reaction, resulting in increased functional properties (Huang et al., 2019). The reduction in the number of hydroxyl groups is responsible for the decrease in the water affinity of GG molecules.

In this study, GG based Pickering emulsion films were prepared with the addition of different amounts of orange peel oil (1 %, 2 % v/v) and glycerol as the plasticizer. The films were stabilized with the incorporation of halloysite nanotubes. Additionally, in order to observe the effect of crosslinking on films' water solubility, a chosen film sample was also crosslinked with STMP. By addition of orange peel oil and halloysite nanotube, the objective is to overcome the biopolymer-based films' main shortcomings, which are the inherently low mechanical strength and water barrier properties. With essential oil incorporation, the films will be given an additional antimicrobial protection function. The overall aim of this study is to assess the performance these applications (oil dispersion, nanoparticle dispersion and crosslinking) in producing films with improved properties and to come up with non-toxic, biodegradable, biopolymer-based, active films that can safely be used as a primary or secondary food packaging material that also has antimicrobial properties.

## 2. Material & methods

### 2.1. Materials

Guar Gum, glycerol (≥%99), orange peel oil (natural, cold-pressed, Brazil origin), sodium trimetaphosphate (STMP, ≥95) and Halloysite nanoclay (30−70 nm × 1−3 μm, nanoclay, powder form) was purchased from Sigma-Aldrich Chemie Gmbh (Darmstadt, Germany). NaOH and HCl, that were also purchased from Sigma-Aldrich Chemie Gmbh (Darmstadt, Germany), were used to adjust the pH of film-forming solutions when necessary.

### 2.2. Preparation of films

Film forming solutions were prepared by dissolving GG (1 % w/v) and glycerol (0.6 % w/v) in Millipore water. To prepare nanodispersions, 1 % (w/v) halloysite nanoclay aqueous mixtures were homogenized by a probe-type ultrasonic homogenizer (750 W, standard probe of 3/4" (19 mm), VCX 750 apparatus, Sonics & Materials, Newtown, CT) operating at 70 % amplitude for 5 min. The concentrations of GG, glycerol and HNT were chosen upon numerous preliminary trials. The concentrations chosen yielded films with the highest physical consistency and mechanical resistance. The prepared halloysite dispersions were added to GG solutions and stirred overnight at 750 rpm using a magnetic stirrer. Orange peel oil (1 and 2 %) was then added to these aqueous dispersions and mixed using a high-speed homogenizer (T25, IKA Co. Ltd., Staufen, Germany) working at 6000 rpm for 5 min. Afterward, the solutions were homogenized using an ultrasonic homogenizer (750 W, VCX 750 apparatus, Sonics & Materials, Newtown, CT) working at 70 % ultrasound amplitude for 10 min with the sample placed inside an ice bath. The resulting film-forming solutions were degassed under vacuum for 20 min to completely remove the bubbles. A measured volume (25 ml) of the prepared solution was then poured onto Petri plates and dried for 96 h under ambient conditions. The obtained films were stored inside desiccators filled with saturated NaBr solutions which provided a controlled relative humidity environment at approximately 50 % relative humidity (%RH). Since physical properties of films are strongly influenced by moisture content, films were removed from desiccators only for analyses.

### 2.3. Experimental design

Upon preliminary trials, optimum GG and glycerol concentrations were chosen as 1% and 0.6 % w/v, respectively. All films contain the same amount of GG and glycerol. Films only varied according to their HNT, oil content, whether they were crosslinked with STMP or not. The final film formulations were given in Table 1. Control films contained only GG and glycerol. Cha films were prepared with halloysite nanoclay addition to control films in order to singularly observe the effect of

**Table 1**
Film Formulations.

| Sample Code | Guar Gum (% w/v) | Glycerol (% w/v) | Halloysite nanoclay (% w/v) | Orange peel oil (% v/v) | Crosslink with STMP |
|---|---|---|---|---|---|
| **Control** | 1 | 0.6 | 0 | 0 | – |
| **CHa** | 1 | 0.6 | 1 | 0 | – |
| **Ha1** | 1 | 0.6 | 1 | 1 | – |
| **Ha2** | 1 | 0.6 | 1 | 2 | – |
| **P-Ha2** | 1 | 0.6 | 1 | 2 | + |

nanodispersed solids on film properties. Ha1 (1 % oil), Ha2 (2 % oil) and P-Ha2 films are emulsion films prepared with the addition of orange peel oil with subsequent ultrasonic homogenization. P-Ha2 differ from Ha1 and Ha2 in that, it additionally went through a phosphate crosslinking protocol via STMP.

### 2.4. Phosphate crosslinking of films

Phosphate crosslinking of GG was carried out according to the method by Gliko-Kabir, Yagen, Penhasi, and Rubinstein (2000). Sodium trimetaphosphate (STMP) dispersion (30 % w/v) was prepared by immersing said amount of STMP into Millipore water and mildly stirring it for 2 h. For complete dispersion of STMP, this step was followed by an ultrasonic homogenization step lasting for 5 min at 70 % power. To decide on the ideal STMP amount for crosslinking, the procedure was performed with increasing amounts of STMP. Phophate groups of STMP will bind to the hydroxyl groups on GG molecules. If there remains free −OH groups after crosslinking, then the procedure is incomplete oppositely if −OH groups are saturated and some phosphate groups are in excess then insoluble STMP particles will decrease film quality. Thus, optimization of STMP amount is an essential step. Five 100 ml GG dispersions adjusted to pH 12 by addition of NaOH, were added 1 ml, 5 ml, 8 ml, 10 ml, 20 ml and 30 ml of 30 % STMP dispersions, which gives 0.1, 0.5, 0.8, 1, 2 and 3 equivalents of STMP, respectively under the assumption that each mole of STMP reacts with three pairs of hydroxyls groups. The reaction mixtures were stirred for an additional 2 h at a maintained pH 12. Final crosslinking STMP concentration was chosen as 0.5 equivalent of STMP upon visual analysis of films. The same procedure was applied to film forming dispersions containing glycerol and halloysite nanoclays with the said STMP concentration to obtain films entitled P-Ha2 (Table 1).

### 2.5. Thickness

Thicknesses of films were measured using a hand-held micrometer (Dial thickness gauge No. 7301, Mitutoyo Co. Ltd., Tokyo, Japan) with 0.01-mm accuracy. Measurements were performed on five different locations on each film (four measurements around the perimeter and one point at the center). Mean thicknesses reported are the average of at least 10 different films.

### 2.6. Density

30 × 30 $mm^2$ square pieces were cut from the films, and the average thickness was determined from three random measurements on these samples. The samples were subsequently dried in an oven at 50 °C for 24 h and weighed. The density was calculated as the ratio of the weight to volume (thickness × area) of the films.

### 2.7. Opacity

The light transmittance of films was measured with a UV–vis spectrophotometer (UV-1700, Shimadzu, Kyoto, Japan), and opacity values were calculated from the Eq. 1;

$$Opacity = \frac{A_{600}}{\delta} \quad (1)$$

where $A_{600}$ is the absorbance at 600 nm and δ is the film thickness (mm) as described by Dick et al. (2015). Three pieces were taken from each film for measurements, and six replicates were measured for each formulation. Greater opacity values represent lower transparencies in films.

### 2.8. Moisture content

Films were pre-conditioned inside desiccators at 50 % RH for 48 h and were subsequently dried inside an oven at 80 °C for 24 h (until the samples reached a constant weight). The moisture content was determined as a percentage of the initial film weight lost during drying and reported on wet basis. Moisture content (%, wet basis) was determined from Eq. 2;

$$\%MC = \frac{Wi - Wf}{Wi} x100 \quad (2)$$

Where *Wi* and *Wf*, are the initial and final weights of the films, respectively.

### 2.9. Water solubility

Square pieces (30 × 30$mm^2$) were cut out from the films and dried in a vacuum oven at 50 °C for 24 h. The dried pieces were weighted and assigned an initial dry weight ($W_{dry,i}$). The pieces were then immersed into 30 ml of distilled water at 25 °C for 24 h. Then, the undissolved remnants were filtered out and subsequently dried at 80 °C for 24 h. The weight of this dried matter was assigned to be the final dry weight ($W_{dry,f}$). Then, the water solubility of films was calculated as follows (Eq. 3);

$$\%WS = \frac{W_{dry,i} - W_{dry,f}}{W_{dry,i}} x100 \quad (3)$$

### 2.10. Fourier-transform infrared (FTIR) analysis

FTIR Spectra of 20 × 20 $mm^2$ pre-dried film samples were acquired using an FTIR spectrophotometer (IR-Affinity1, Shimadzu, Kyoto, Japan) in attenuated total reflectance (ATR) mode using a diamond ATR crystal. The infrared regions' analyses were recorded with 32 scans over the wavenumber range of 600–4000 $cm^{-1}$.

### 2.11. Contact angle

To estimate the wettability of the films, 10−15 μl droplets of Millipore water was deposited on the film surface. Using a Kruss DSA100 Instrument (KRÜSS GmbH, Hamburg, Germany) a magnified image of the drop profile was conveyed to a computer, allowing measurement of the changes in droplet shape to be recorded as digital images over time. The contact angle was measured between the baseline of the drop and the tangent at the drop boundary. The image processing and curve fitting for contact angle measurement was carried out from a theoretical meridian drop profile carried out by the software DSA version 1.90.0.11. Since the films were highly soluble in water, the measurements were performed within the first 10 s after dropping distilled water onto film surfaces.

### 2.12. Antimicrobial activity

Antimicrobial activity was examined using inhibition zone assay in agar medium as described by Meira et al. (2017). Pieces from the films (1 cm diameter) were cut and placed on Lysogeny broth (LB) agar plates. Then, 10 ml LB soft agar (7.5 g/l) were inoculated with 250 μl of strains *Escherichia coli* (indicator for Gr−) or *Bacillus subtilis* (indicator for Gr+) ($10^7$ cfu/mL). Then, the mixtures were poured onto petri dishes. Plates were incubated at 37 °C for 24 h to promote microorganism growth. The antimicrobial activity was evidenced by clear zones (no microorganism growth or survival) surrounding film pieces. The diameter of the inhibition zones was measured and reported in mm. Measurements were taken in 5 replicates.

In order to investigate the effect of films on preserving food quality, strawberries purchased from a local grocery store were placed on films

and kept at ambient conditions (25 °C and 40 % RH). The fruits were photographed every day and visually analyzed for quality deterioration and possible mold growth.

### 2.13. Water vapor permeability (WVP)

WVP of films were determined using a modified version of ASTM E-96 method (Bertuzzi, Castro Vidaurre, Armada, & Gottifredi, 2007). Cylindrical test cups custom manufactured out of polyacetal (Delrin) with 40 mm internal diameter were filled with 30 ml of distilled water. Films were placed on top of cups and caps were screwed tight with a rubber joint placed between the film and the cap to ensure that water vapor only permeated through the films. Mass transfer occurs through the film section that resides within the inside of the cups and has an area of 12.5 $cm^2$. A schematic representation of the cups is given in Fig. 1. These test cups were placed into pre-equilibrated 15–20 % RH desiccator cabinets. Films were assumed to be subjected to 100 % RH on the inside with the outside %RH and temperature being measured with an electronic RH sensor. Each film was weighed at least 10 times with 2 h breaks between each measurement. The water vapor transmission rates (WVTRs; g $m^{-2}$ $s^{-1}$) were determined from the slope of the weight loss *versus* time. WVP was calculated from the Eq. 4;

$$WVP\ (g \cdot m^{-1} \cdot s^{-1} \cdot Pa^{-1}) = \frac{WVTR \times \Delta x}{P_{w,i} - P_{w,o}} \quad (4)$$

where $\Delta x$ is the film thickness, $P_{w,i}$ is the partial pressure of water vapor at the inner surface of the film inside the cup (Pa) and $P_{w,o}$ is the partial pressure of the water vapor at the outer surface of the film outside the cup (Pa). Measurements were performed in triplicates.

### 2.14. Mechanical properties

The mechanical properties were measured with a universal testing machine (Z250, Zwick/Roell, Ulm, Germany) at 25 mm/min with a load cell of 1 kN. The film samples were mounted in the film-extension grips with a grip- to-grip separation of 25 mm. The tensile strength at break (TS) and percentage elongation at break (EAB) were calculated as follows (Eqs. 5 and 6);

$$TS = \frac{F_{max}}{A} \quad (5)$$

$$EAB = \left(\frac{L}{L_0}\right) \times 100 \quad (6)$$

where $F_{max}$ is the maximum load for film rupture (N), $A$ is the cross-sectional area of the sample. $L_0$ represents the initial gage length (25 mm) of the sample, $L$ the final length of the film before the moment of rupture (Acevedo-Fani et al., 2015). Young's modulus is described as the slope of the initial linear section of the stress-strain curve (Liu et al., 2018) and was from Eq. 7;

$$YM = \frac{\sigma_2 - \sigma_1}{\varepsilon_2 - \varepsilon_1} \quad (7)$$

Where $\varepsilon_1$ is a strain of 0.1, $\varepsilon_2$ is a strain of 0.15, $\sigma_1$ (MPa) is the stress at $\varepsilon_1$, and $\sigma_2$ (MPa) is the stress at $\varepsilon_2$. Five replicates were taken per formulation.

### 2.15. Statistical analysis

Statistical analyses were performed using statistical analysis software (Minitab v16.0, Pennsylvania, USA). For comparison of the means to identify which groups were significantly different from others, analysis of variance (ANOVA) with Tukey's multiple comparison test was used. Differences were considered significant for $p < 0.05$. All data are presented as the mean (of at least four measurements) ± standard deviation.

## 3. Results & discussion

### 3.1. Density and thickness

Visually, all of the films displayed a homogenous surface with no bubbles or cracks. They also possessed satisfactory handling characteristics and could easily be detached from the Petri dishes without tearing. Photos of films were presented in Fig. 2. Densities of the films ranged between 0.68 ± 0.01 and 0.91 ± 0.02 g $cm^{-3}$ (Table 2). This is lower than most flour, starch or protein films, such as cassava starch films (around 1.35 g $cm^{-3}$) (Gutiérrez, Morales, Pérez, Tapia, & Famá, 2015), keratin films (0.92–1.10 g $cm^{-3}$) (Rocha Plácido Moore, Maria Martelli, Gandolfo, José do Amaral Sobral, & Borges Laurindo, 2006), rice flour films (1.13–.140 g $cm^{-3}$) (Dias, Müller, Larotonda, & Laurindo, 2010), banana flour (0.94–1.25 g $cm^{-3}$) (Pelissari, Andrade-Mahecha, Sobral, & Menegalli, 2013a). Density is controlled by internal film structure and changes with the composition, molecular weight, and interactions

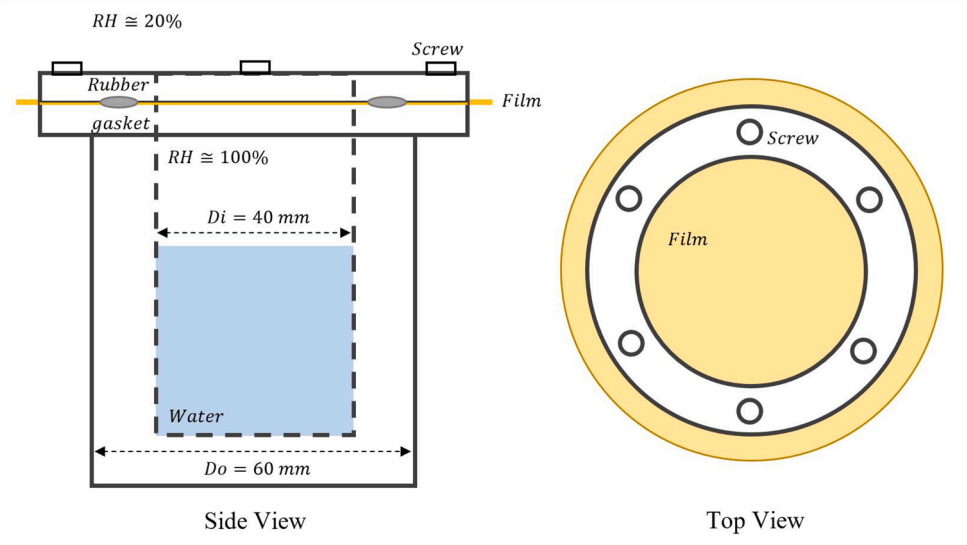


**Fig. 1.** Schematic representation of WVP measurement cups.

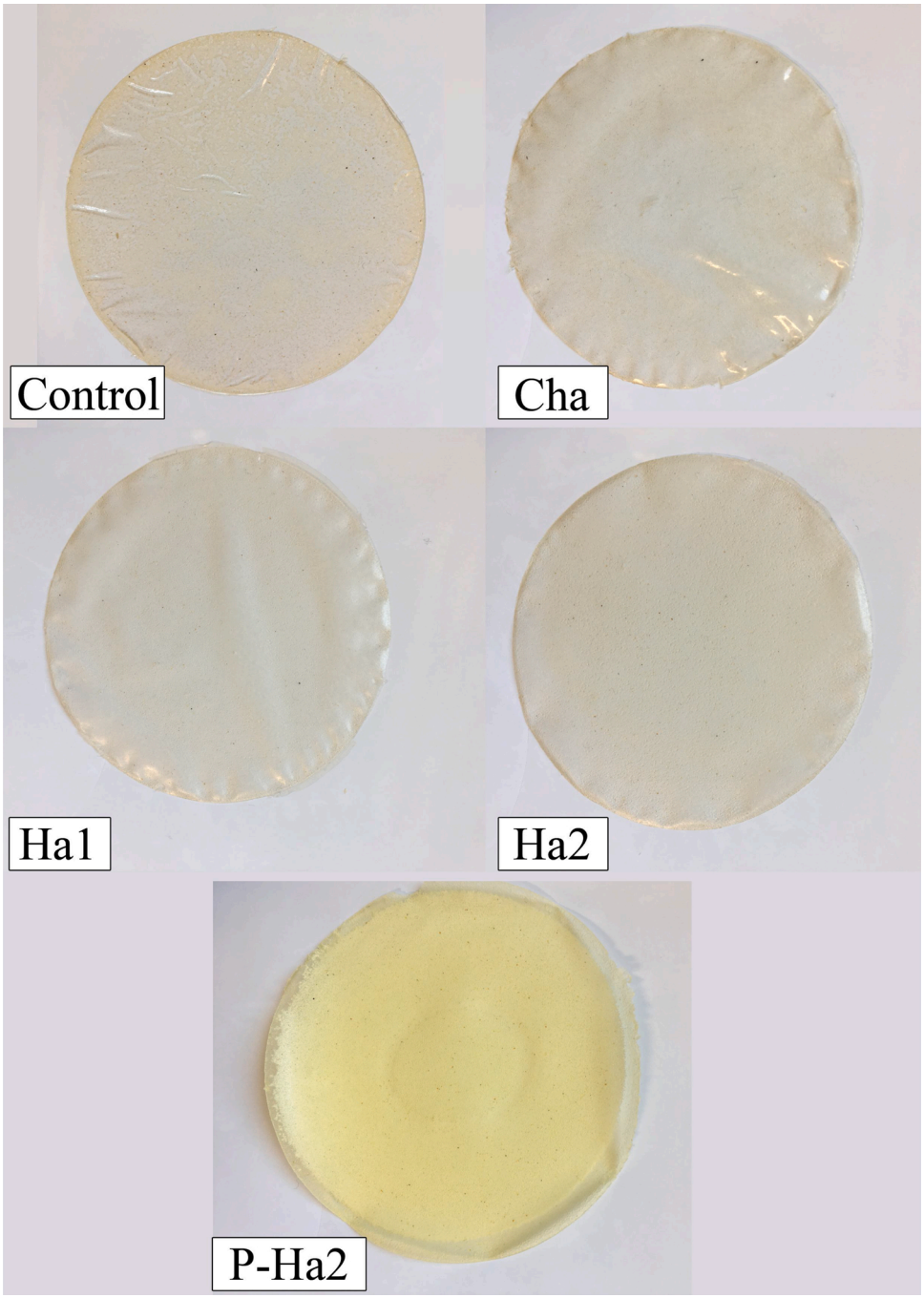


**Fig. 2.** Images of film specimen.

**Table 2**
Physical characteristics of GG film samples.

| | Density (g/cm$^3$) | Moisture Content (%) | Solubility (%) | Opacity | WVP x10$^{-9}$ (g m$^{-1}$ s$^{-1}$ Pa$^{-1}$) | Contact angle (°) | Thickness (mm) |
|---|---|---|---|---|---|---|---|
| **Control** | 0.68 ± 0.01$^{c}$ | 34.85 ± 1.18$^{a}$ | 79.88 ± 0.72$^{a}$ | 4.05 ± 0.15$^{d}$ | 3.861 ± 0.022$^{a}$ | Not applicable | 0.068 ± 0.001$^{d}$ |
| **Cha** | 0.81 ± 0.01$^{b}$ | 31.14 ± 0.53b | 70.75 ± 1.50$^{b}$ | 5.08 ± 0.12$^{c}$ | 2.995 ± 0.135$^{b}$ | 33.84 ± 0.58$^{c}$ | 0.089 ± 0.001$^{c}$ |
| **Ha1** | 0.78 ± 0.01$^{b}$ | 22.35 ± 0.48$^{c}$ | 61.68 ± 1.01$^{c}$ | 8.53 ± 0.24$^{b}$ | 2.596 ± 0.042$^{b}$ | 48.35 ± 0.23$^{b}$ | 0.113 ± 0.002$^{b}$ |
| **Ha2** | 0.80 ± 0.01$^{b}$ | 20.76 ± 0.19$^{cd}$ | 59.04 ± 1.17$^{c}$ | 9.24 ± 0.19$^{b}$ | 2.083 ± 0.132$^{c}$ | 56.74 ± 0.36$^{a}$ | 0.135 ± 0.003$^{a}$ |
| **P-Ha2** | 0.91 ± 0.02$^{a}$ | 18.57 ± 0.22$^{d}$ | 58.39 ± 0.87$^{c}$ | 21.92 ± 0.40$^{a}$ | 1.752 ± 0.014$^{c}$ | 48.54 ± 0.54$^{b}$ | 0.121 ± 0.001$^{b}$ |

Means within the same column, followed by the different letters (a–d) are significantly different ($p < 0.05$).

between the components present in the films a (Pelissari, Andrade-Mahecha, Sobral, & Menegalli, 2013b). Dispersal of halloysite nanoclay into the films increased the density significantly ($p < 0.05$), whereas oil concentration had no effect on it (Table 2). Crosslinking also yielded films with significantly increased densities. Increased number of interactions between molecules due to crosslinking, likely modified the

polymer network to result in a tighter molecular packing.

Film thicknesses ranged from 0.068 to 0.135 mm. Film thickness is a function of the type and concentration of the biopolymer and/or the additives incorporated (Meira et al., 2017). Both HNT and orange peel oil addition led to significantly increased film thicknesses ($p < 0.05$). The increased solid content with halloysite addition could be the result of the increased thickness. Similarly, nanoclay addition was reported to increase film thicknesses in some other studies (Lee et al., 2018; Meira et al., 2017). The increase in thicknesses with orange peel oil incorporation or an increase in oil concentration, was in accordance with the findings from other previous studies (Lee et al., 2018; Ma et al., 2015; Ojagh, Rezaei, Razavi, & Hosseini, 2010). Oil due to being thermodynamically incompatible with the aqueous polymer phase, likely increased the distance between molecules, thereby leading to thicker films. Crosslinking, on the other hand, significantly decreased film thickness, which was associated with a tighter packing of molecules as previously mentioned.

### 3.2. Opacity

Transparency is of vital importance in consumer preference since it has a direct impact on the appearance of the packaged product. Opacity values are listed in Table 2 and images of films were provided in Fig. 2. Apart from the crosslinked sample (P-Ha2), the films can be considered quite transparent (with opacity values ranging between $4.05 \pm 0.15$ and $9.24 \pm 0.19$ $mm^{-1}$). This is close to the 4.26 $mm^{-1}$, which is the opacity of polyethylene films (Galus, 2018). Opacity can be an essential factor in determining an appropriate application for the films. Films with low opacity values like the ones reported are more suitable for foods that could benefit from direct visibility through the wrapping. Opaque films, on the other hand, provide protection against incident light for products that are sensitive to light catalyzed degradation reactions such as lipid oxidation (Aydogdu, Kirtil, Sumnu, Oztop, & Aydogdu, 2018). Control films made solely of GG and glycerol displayed the highest transparency. Dispersion of halloysite nanotube significantly increased the opacity of films ($p < 0.05$). This is to be expected as solid particles dispersed in a liquid scatter light and cause the resulting dispersion to appear turbid (Anal, Shrestha, & Sadiq, 2019). Similar findings were witnessed in multiple previous studies (Lee et al., 2018; Meira et al., 2017; Yin et al., 2015).

Orange peel oil incorporation to Cha films increased opacity by 68 %. The increase of oil content from 1 to 2 % v/v also resulted in an increase in opacities, though the difference was not statistically significant ($p > 0.05$). The increasing opacity with oil addition was reported in numerous other studies with emulsion films (Azeredo et al., 2017; Fernández, De Apodaca, Cebrián, Villarán, & Maté, 2007; Galus & Kadzińska, 2016; Pereda, Amica, & Marcovich, 2012; Wang et al., 2014). This behavior is attributed to promoted light scattering as a result of the dispersion of a secondary immiscible phase with a different refractive index into the primary hydrocolloid matrix (Galus, 2018).

Crosslinked films (P-Ha2) displayed much higher opacities than all other films which could easily be distinguished by visual inspection (Fig. 2). This high opacity indicates films could provide excellent protection against UV light, which would make them suitable for use with foods susceptible to light-induced lipid oxidation (Lee et al., 2018; Lei et al., 2019). The extensive bonds formed by crosslinking most likely decreased the distance between polymer chains, making the film structure more compact and therefore reducing the light that can pass through the films. Numerous other studies have also reported an increased opacity with crosslinking (Costa et al., 2018; Fan, Duquette, Dumont, & Simpson, 2018; Li, Zhu, Guan, & Wu, 2019).

### 3.3. Moisture content & solubility

Packaging films are likely to be in contact with foods of high moisture content. Therefore, measurement of moisture content and total soluble matter that act as an indicator of film hydrophilicity, is of utmost importance (Singh, Chatli, & Sahoo, 2015). Moisture contents of films ranged from 18.6 to 34.8 %. Out of the film samples, control ones held the highest amount of moisture after drying (Table 2). Crosslinking and addition of oil or HNT particles into the films each decreased the moisture content. Presence of HNT particles in the film matrix as well as increasing the overall solid content also inhibited water absorption which explains the decreased moisture content. HNT addition was confirmed to decrease moisture content of films in previous studies (Casariego et al., 2009; Lee et al., 2018). Addition of orange peel oil also decreased moisture content significantly ($p < 0.05$). We have also observed a slight decrease in mean moisture content with increasing oil concentration, but it was not statistically significant ($p > 0.05$). Hydroxyl groups on the orange peel oil, presumably, formed hydrogen bonds with the polar GG molecules which decreased the availability of hydroxyl groups to interact with water molecules. Lee et al. (2018) also reported similar results for chitosan-based emulsion films. Crosslinking of GG with STMP molecules, similarly, decreased the available −OH groups to hydrogen bond with water, which caused a decrease in films water holding capability.

As shown in Table 2, films were highly water soluble, which was not surprising considering the profoundly hydrophilic character of GG and glycerol, which forms the basis of the films. HNT and oil dispersion into films though were effective in decreasing solubility. Presence of solid nanoparticles kept the film structure more intact, even when dispersed in water, by decreasing direct contact of water with the GG molecules. Oil addition, on the other hand, increased the hydrophobic character of film solutions, as a result, decreased films water solubility. Crosslinking, much to our surprise, was not successful in decreasing water solubility. Free −OH groups seem to have decreased as illustrated by FTIR curves (Fig. 3), yet this apparently was not enough to lower films' water solubility. The result of this could be related to the concentration of STMP used. 0.5 equivalent chosen after preliminary trials could be too high for the −OH groups present in the films. This means that some of the STMP could have left unbonded in salt form, which could have compensated for the decreased −OH availability by providing water with more polar groups to interact with. Gutiérrez, Guzmán, Medina Jaramillo, and Famá (2016) for similar reasons, measured increased water solubilities after phosphate crosslinking of cassava starch films (Gutiérrez et al., 2016).

### 3.4. Fourier-transform infrared (FTIR) spectroscopy

Nano and microstructural changes could occur due to polymer interactions in the blends, which can become prominent in the final structural properties of the film. FTIR analyses enable the examination of particular interactions between functional groups of the chains which can be observed as shifts in the chain's specific IR bands (Aydogdu et al., 2018). FTIR spectra of all films were given in Fig. 2.

Control films (with GG and glycerol only) showed some distinct absorption bands: at the region from 3650 to 3000 $cm^{-1}$ which is commonly associated with the stretching vibration of O—H bond (Borges et al., 2013; Lei et al., 2019), in the region 3000−2800 $cm^{-1}$ that is attributed to CH— bond stretching (Cano et al., 2015; Gutiérrez et al., 2016), centered around 1645 $cm^{-1}$ which is related to bending vibration of O—H (Borges et al., 2013; Meira et al., 2017), centered around 1370 $cm^{-1}$ that refer to the stretching of Amide III band coming from the protein in the gum (GG contains 5 % by wt. proteins) (Pelissari et al., 2013b; Verma & Sharma, 2021), reaching from 1200 to 900 $cm^{-1}$ centered around 1053 $cm^{-1}$ which corresponds to stretching vibration of C—OH— bonds which the film had in abundance due to GG being a galactomannan polymer (Cano et al., 2015; Meira et al., 2017; Pelissari et al., 2013b).

With HNT or orange peel oil addition, the changes observed in FTIR Spectra were hard to distinguish, possibly related to the low concentration range employed (1–2 %). Absence of any new peak formation

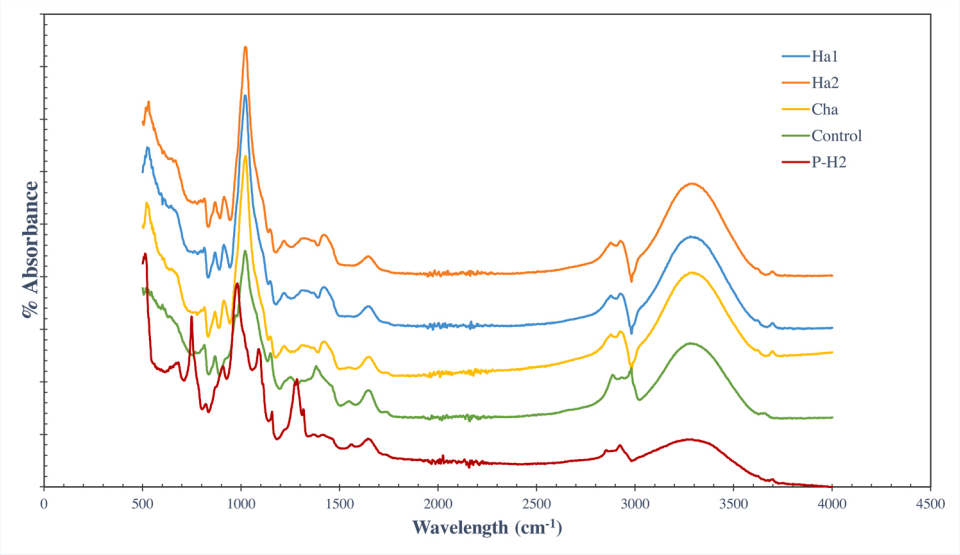


**Fig. 3.** FTIR spectra of GG films.

demonstrate that no new bonds were formed between orange peel oil, HNT and GG /glycerol matrix. The only changes were minor peak formations centered around 905 $cm^{-1}$ and 1419 $cm^{-1}$ which is generally attributed to phosphorous stretching (P—OP) and CH—— bending, respectively (Borges et al., 2013; Variyar et al., 2015). P—OP— stretching band can be observed in nano-composite films due to presence of nanoclays (Variyar et al., 2015). Formation of a C—H bending peak, was related to an increase in the number of aliphatic chains bonded through single carbon-carbon bonds, which oils have in abundance. Crosslinking, on the other hand, substantially changed the overall appearance of FTIR spectra with the most dominant change being the drop in O—H stretching band intensity. This points out to a decrease in the free O—H groups. As previously mentioned, STMP links to GG molecules through the free hydroxyl groups. There was also formation of a new band at 1275 $cm^{-1}$, which could be associated with phosphate vibration (P═O) (Yıldırım-Yalçın et al., 2019). This obvious drop in O—H bond intensity coupled with phosphate bond formation, indicates that crosslinking of GG with STMP was successful.

### 3.5. Wettability

Surface water wettability is essential in assessing coating and food compatibility. Wettability usually involves the measurement of contact angles (CA) as the primary data. It consists of measuring the angle formed at the three-phase contact line where liquid, gas and solid phases intersect. Low contact angles correspond to high wettability which is an indicator for higher hydrophilicity. The hydrophilic and hydrophobic regimes are distinguished by a 90° angle. The liquid is considered to be wetting the solid, if CA $< 90°$ and non-wetting if CA $> 90°$ (Aphibanthammakit, Nigen, Gaucel, Sanchez, & Chalier, 2018; Kowalczyk et al., 2016).

CA data can be viewed in Table 2. Control films were highly soluble in water (71 % soluble in water, see Table 2), so much so that the films dissolved within a few seconds of droplet deposition on films. Despite our continuous efforts, reliable data could not be received. Therefore, no data could be acquired for the highly hydrophilic control sample. All remaining measurements were taken for the initial 10 s after droplet deposition. There was no substantial deviation in CAs during data acquisition. Despite the solubility of all other films being relatively close to control films, the resistance of film surface against water exposition was much higher in all the other samples. This could be associated with the difference between films' bulk and surface properties (Svitova, Leung, & Lin, 2010). Films with the lowest CA were control films containing halloysite nanoclay (Cha). This indicates that out of the samples prepared, Cha has the highest water wettability which means it has the lowest surface hydrophobicity. Despite its high hydrophilicity, nanofiller fortified films showed some resistance against water deposition. These water-insoluble nanotube silica particles, most likely, provided a barrier on the surface of the film and reduced the interaction of water with the abundant hydroxyl groups of highly soluble GG and glycerol molecules. Similarly, other researchers have also reported decreased CAs with the dispersion of HNT or other nanoparticle fillers (Lee et al., 2018; Liu, Wang, Qi, Huang, & Xiao, 2019).

With orange peel oil content, contact angles, expectedly, increased from 33.84 ± 0.58 (for Cha films) to 48.35 ± 0.23 with 1 % and to 56.74 ± 0.36 with 2 % oil addition. It is typical for the film surface to display enhanced hydrophobicity with increased oil concentration. Several other studies have reported a similar result with essential oil addition to films (Atef, Rezaei, & Behrooz, 2015; Bahram et al., 2014; Lee et al., 2018; Ojagh et al., 2010). Crosslinking significantly increased surface water wettability (P-Ha2 from Table 2). sodium Triphosphate addition and phosphorylation of GG molecules leads to extensive bonding and a more compact structure which most likely acted against agglomeration and floatation of oil droplets to film surface. This, in turn, retarded formation of a more hydrophobic layer on the film surface (Sgorla et al., 2016).

### 3.6. Antimicrobial properties

To assess antimicrobial efficiency of orange peel oil in films, pieces from three film samples (Cha as control, Ha1 and Ha2) were placed onto Petri dishes with Gr− (*E. coli*) and Gr+ (*B. subtilis*) bacteria. Inhibition zones were measured and images were acquired (Fig. 4). In addition to inhibition zone analysis, strawberries were placed on the films and left at ambient conditions for days to evaluate films effectiveness in increasing the shelf life of a real food. These images were given in Fig. 5.

As expected, control films (Cha) not exhibit any growth inhibition on Gr− or Gr+ bacteria. Films with 1 % and 2 % orange peel oil both showed antimicrobial properties against Gr− and Gr+ bacteria. However, by 2 % oil addition, inhibition zone diameter increased considerably for Gr− bacteria (from 1.91 ± 0.07 in Ha1 to 2.44 ± 0.15 cm in Ha2). For Gr+ bacteria, the inhibition zone sizes were smaller (2.02 ± 0.04 cm in Ha1 and 2.12 ± 0.12 cm in Ha2). These results confirm that orange peel oil preserves its antimicrobial activity inside the films. Bacteriostatic effects of essential oils incorporated into films were previously demonstrated in a number of studies (Acevedo-Fani et al., 2015;

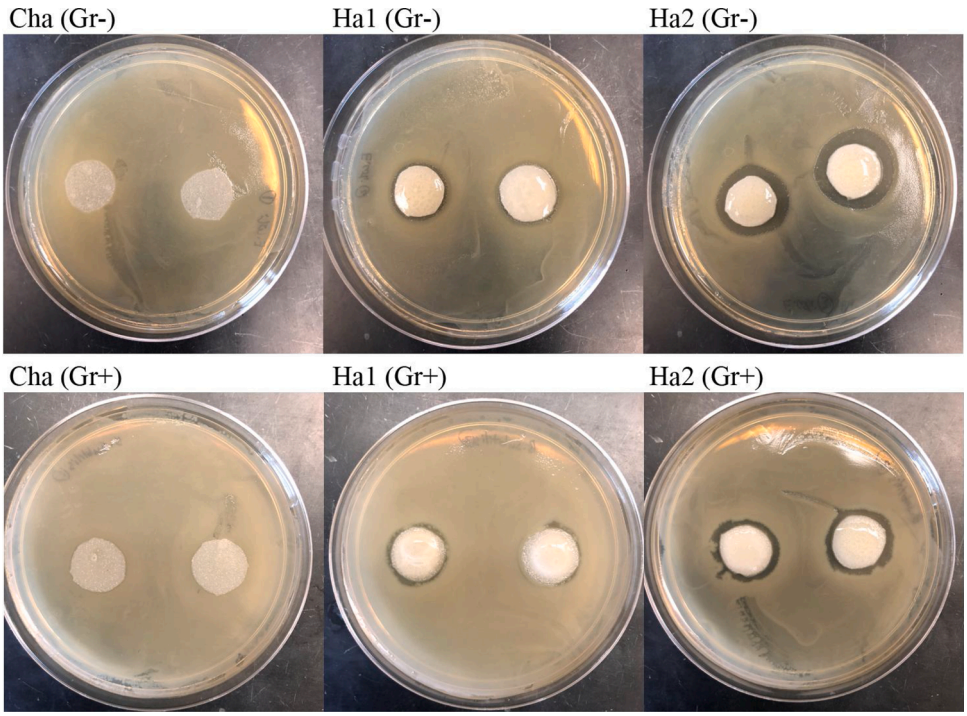


**Fig. 4.** Images of bacterial culture plates incubated with GG films. (Top) *E. coli* cultures (Bottom) *B. subtilis* cultures.

Ke et al., 2019; Lei et al., 2019; Meira et al., 2017; Wu et al., 2019). This effect is associated with the damage of essential oils to cell membranes. Gram – bacteria were more susceptible to inhibition by orange peel oil compared to Gram+ bacteria. This finding was previously explained by more effective transportation of essential oils into the Gr− bacteria via outer membrane transporters on the cell membrane (Ke et al., 2019).

Strawberry images can be seen in Fig. 5. For these measurements, strawberries were chosen for their high perishability. Strawberries have a high water content and relatively low sugar content compared to most fruits, which grant it a higher water activity (Lequeu, Fauconnier, Chammaï, Bronner, & Blée, 2003; Ragaert, Verbeke, Devlieghere, & Debevere, 2004). As observed in Fig. 5, visual examination of strawberry spoilage yielded results that were in agreement with antimicrobial activities of films. Between Day 0 and Day 6, there wasn't much difference in the visual appearance strawberries other than an expected loss in quality such as shrinkage due to water loss and decolorization due to pigment oxidation (Fennema, 1996). On Day 7, we have observed some mold growth on strawberries placed on Control and Ha1 films, yet no such visible growth on Ha2 films. On Day 9, all strawberries displayed visible signs of mold growth. However, strawberries on Ha1 and Ha2 films seemed to have less mold growth. This indicated that films do not have to be in direct contact with the whole food surface to retard microbial growth. Essential oils (EOs) are known to be volatile which explains how they show antimicrobial activity without necessitating direct contact. However, direct addition would not provide prolonged antimicrobial activity, as EOs would evaporate at a faster rate. Incorporation of EOs into halloysite reinforced GG/glycerol polymer matrix provides controlled release of EOs. Many studies have used biopolymeric films for delivery of active ingredients (Gomaa et al., 2018; Ke et al., 2019; Kowalczyk et al., 2016).

### 3.7. Water vapor permeability

Control of moisture transfer between the food and its environment, or different parts of a multi-component food is the most fundamental function of food packaging, particularly owing to the dominant influence of water on the rate of deteriorative reactions (Ahmadi, Kalbasi-Ashtari, Oromiehie, Yarmand, & Jahandideh, 2012; Gontard, Guilbert, & Cuq, 1992). As a result, water vapor permeability (WVP) is the most extensively studied property of edible films (Singh et al., 2015). Relative humidity (RH) of the film's environment directly affects the WVP of films. WVPs are increased as films are kept at higher RH's (Chang & Nickerson, 2015). WVP's reported in Table 2 are of GG films preserved at a controlled atmosphere of 25 °C and 50 % RH. WVPs of films ranged between $1.752 \pm 0.014^{c}$ and $3.861 \pm 0.022^{a}$ ng $m^{-1}$ $s^{-1}$ $Pa^{-1}$, with control films showing the highest WVP out of all. This means orange peel oil incorporation, HNT dispersion and crosslinking were all effective in reducing films WVPs. Minimization of films' WVPs is almost always preferable with the exception of packages to be used in unpeeled fresh fruits or vegetables that need to dispose of water built on by respiration during storage. In that regard, biopolymer-based films could be a good alternative to low-density polyethylene (LDPE) bags which has a much lower WVP ($0.036 \cdot 10^{-2}$ ng $m^{-1}$ $s^{-1}$ $Pa^{-1}$) (Mali, Grossmann, Garcia, Martino, & Zaritzky, 2004). The range of WVP we observed with GG films lied somewhere in the middle compared to other biopolymer films in literature. They were superior compared to films composed of just one hydrophilic polymer such as potato peel films (2.99–5.6 ng $m^{-1}$ $s^{-1}$ $Pa^{-1}$) (Kang & Min, 2010) and whey protein isolate films (5.16 ng $m^{-1}$ $s^{-1}$ $Pa^{-1}$) (McHugh, Avenabustillos, & Krochta, 1993), yet weaker compared to bio-composite films, like banana flour films (0.200 ng $m^{-1}$ $s^{-1}$ $Pa^{-1}$) (Pelissari et al., 2013b) and lentil flour films ($0.245 \pm 0.042$ and $0.352 \pm 0.048$ ng $m^{-1}$ $s^{-1}$ $Pa^{-1}$) (Aydogdu et al., 2018).

WVP of films decreased with HNT addition. HNT, being an aluminosilicate mineral, is itself impermeable to water vapor, other gases and aroma compounds (Lee et al., 2018), and when it is dispersed into films, it creates a tortuous pathway for the diffusion of water and gas molecules, thereby increasing the mean path lengths for molecules to pass through (Casariego et al., 2009; Variyar et al., 2015). This behavior explains the reason for reduced WVP with HNT dispersal. Numerous studies in literature have also reported decreased WVPs with dispersion of HNTs or other nanoclays (Benbettaïeb et al., 2016; Casariego et al., 2009; Lee et al., 2018; Liu et al., 2019; Variyar et al., 2015). Orange peel oil also significantly decreased WVP (13 % decrease in Ha1 films, 30 %

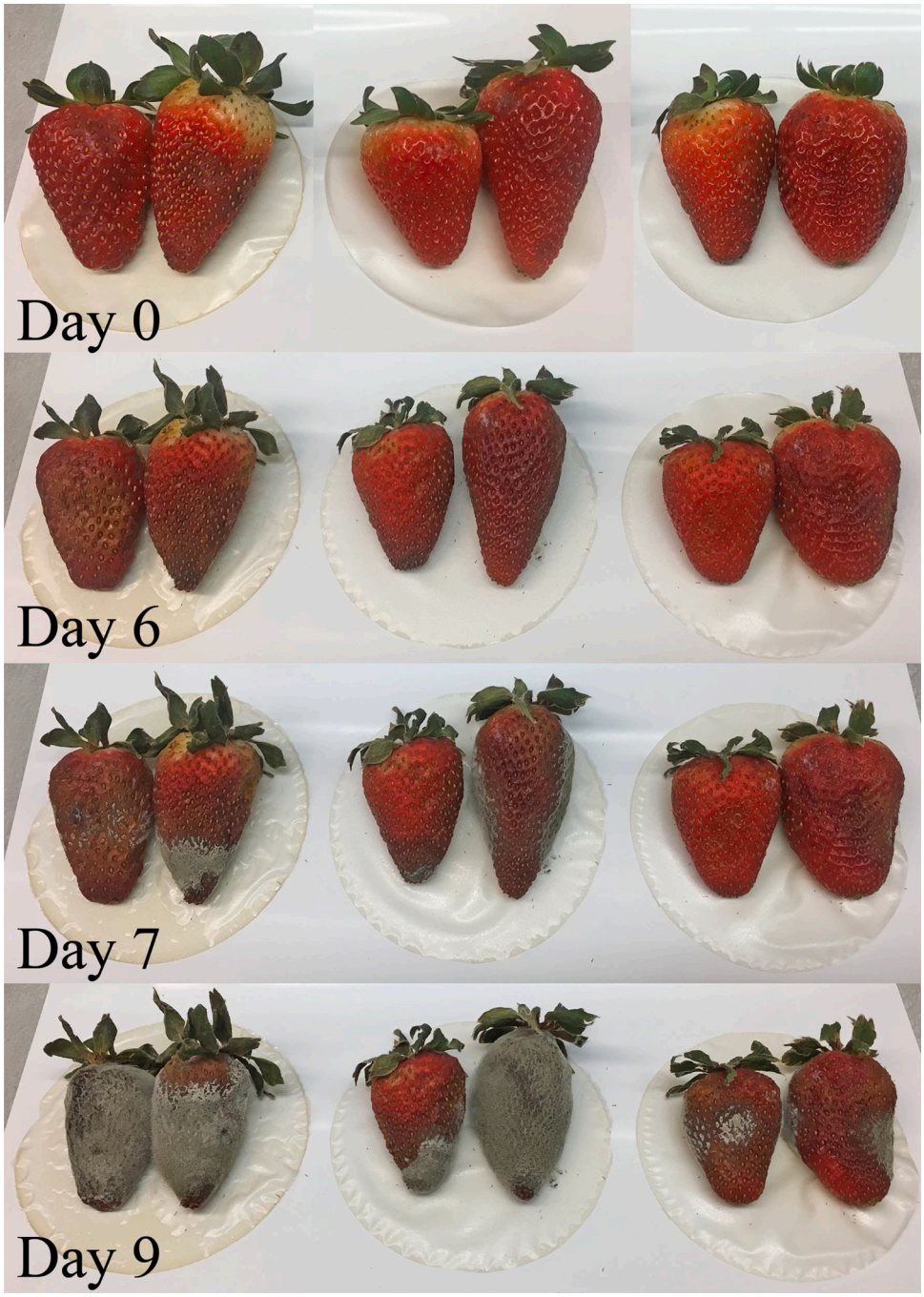


**Fig. 5.** Images of strawberries deposited on GG films taken over the course of 9 days. From left to right, the film samples are Control, Ha1 and Ha2, respectively.

decrease in Ha2 films). The transport of moisture is carried out by the hydrophilic fraction of the films, that's why permeability strongly depends on the films' hydrophilic-lipophilic ratio (Hernandez, 1994). The diffusion of water vapor is slower when oil phase concentration is increased or oil particle sizes are reduced (Acevedo-Fani et al., 2015). The increased hydrophobicity of films with orange peel oil addition seemed to have retarded the transfer of water vapor through the films. By crosslinking with STMP, films seemed to have improved water barrier properties as seen in Table 2. Crosslinking by extensively bonding polymer chains to one another restricts the mobility of water (Yıldırım-Yalçın et al., 2019). Additionally, it also decreased the number of free −OH groups that interact with the water molecules which was also supported by FTIR spectra (Fig. 2). As shown in Fig. 2, crosslinked films have much lower intensities in the regions between 3000–3500 $cm^{-1}$, commonly associated with stretching of O—H bonds. Similar results were reported in previous studies (Sgorla et al., 2016; Yıldırım-Yalçın et al., 2019)

### 3.8. Mechanical properties

The most fundamental function of food packaging is to assure continual mechanical protection of the food by helping it preserve its structural integrity. Thus, for almost all types of applications, films with good mechanical resistance that provides the food with some resistance against deformation is preferable (Gontard et al., 1992). Poor mechanical properties compared to synthetic polymers remains to be the limiting factor in the commercial use of biopolymer-based films (Wu et al., 2019). The most common parameters that describe the

mechanical properties of edible films are tensile strength (TS), elongation at break (EAB) and Young's modulus (YM). Tensile strength is the maximum stress that a material can withstand before breakage. Elongation at break is the percent elongation of the film with respect to its initial length and is a measure of materials stretching capability. Young modulus, or elastic modulus, is an indication of the film's rigidity (Acevedo-Fani et al., 2015; Variyar et al., 2015). Film's mechanical measurement results were presented in Table 3. Films displayed relatively low TS values and much higher elongation values compared to most other biopolymer-based films (Acevedo-Fani et al., 2015; Azeredo et al., 2017; Galus, 2018; Ke et al., 2019; Lee et al., 2018; Meira et al., 2017; Musso, Salgado, & Mauri, 2017; Yin et al., 2015). TS of most of the samples were higher than the acceptable value of 4 MPa for food packaging purposes (Tajeddin, Rahman, & Abdulah, 2010).

According to these results, HNT addition had no significant effect on the film's tensile properties ($p > 0.05$). This could be related to poor optimization of halloysite nanoclay content and its homogenization procedure. Previous studies using halloysite content and homogenization time/strength as the main parameters in edible films, showed that choice of an ideal HNT concentration and homogenization method parameter combination is necessary for optimal nano-reinforcement of films (Lee et al., 2018; Nascimento, Calado, & Carvalho, 2012; Variyar et al., 2015). A more than optimal HNT concentration or improper homogenization could lead to agglomeration of clay particles leading to the generation of stacked clays through the polymer matrix. This could cause damages and cracks in the films that disrupt film matrix cohesiveness (Lee et al., 2018; Variyar et al., 2015). Too much homogenization, on the other hand, could break the nanotubes and result in a reduction in their aspect ratio, which also negatively affect mechanical properties (Hussain, Chen, & Hojjati, 2007).

Dispersion of orange peel oil into films significantly decreased films' mechanical resistance. While it did not seem to affect EAB's much, it decreased tensile strengths almost by half. Some researchers have found essential oil to display plasticizer properties, which is strongly dependent on the type of polymers that surround the essential oil (Azeredo et al., 2017; Ke et al., 2019). In our case, the plasticizer effect was not observed, as TS decrease was not accompanied by increased EAB's. Oil droplets could act as structural defects in the continuous polymer matrix which promotes crack formation. Microcracks inside the films act as initiation points for film breakage during stretching, which consequently weakens films' mechanical resistance (Azeredo et al., 2017). YM of films also decreased with increasing oil concentration, which also points out to a weakening in the film structure. Many studies have reported similar findings in biopolymer-based films (Azeredo et al., 2017; Ke et al., 2019; Yin et al., 2015; Zúñiga, Skurtys, Osorio, Aguilera, & Pedreschi, 2012). STMP crosslinked film (P-Ha2) despite having a marginal influence on TS, reduced films EAB's down to 30 % (P-Ha2) from 73.5 % (Ha2). Conversely, YM of films increased from $3.76 \pm 1.04$ MPa to $9.46 \pm 1.25$ MPa with crosslinking. This was to be expected, as crosslinking agents tend to have an anti-plasticizer effect in the sense that, opposite to plasticizers they restrict polymer chain mobility (Borges et al., 2013). Yıldırım-Yalçın et al. (2019) also found a slight increase in TS accompanied by a sharp decrease in EAB in STMP crosslinked GG films.

**Table 3**
Tensile properties of films.

| | Tensile Strength (MPa) | Elongation at break (%) | Young's Modulus (MPa) |
|---|---|---|---|
| **Control H** | $5.34 \pm 0.30^{a}$ | $64.75 \pm 0.86^{b}$ | $8.92 \pm 1.00^{a}$ |
| **Cha** | $5.67 \pm 0.28^{a}$ | $70.24 \pm 1.29^{ab}$ | $8.23 \pm 1.12^{a}$ |
| **Ha1** | $3.73 \pm 0.10^{b}$ | $78.52 \pm 1.61^{a}$ | $4.84 \pm 1.15^{b}$ |
| **Ha2** | $2.35 \pm 0.11^{c}$ | $73.55 \pm 4.71^{ab}$ | $3.76 \pm 1.04^{b}$ |
| **P-Ha2** | $3.31 \pm 0.13^{b}$ | $30.30 \pm 1.24^{b}$ | $9.46 \pm 1.25^{a}$ |

Means within the same column, followed by the different letters (a–c) are significantly different ($p < 0.05$).

## 4. Conclusion

The aim of the study was to investigate the effectiveness of commonly applied methods to improve biopolymer-based films' properties that still seem to be lagging much behind synthetic polymers. Reinforcement with nano-fillers and dispersion of orange peel oil into films, or crosslinking with STMP were shown to be promising strategies. Different film specimen had largely distinct visual properties, with widely different transparencies; with widely diverse transparencies (with opacity values ranging between $4.05 \pm 0.15$ and $9.24 \pm 0.19$ $mm^{-1}$). The distinct variance between different samples was also reflected in other film properties such as water solubility and surface wettability (providing a dissolvability range from 58 % to 80 % and water contact angles between 34°–57°). Orange peel oil and/or HNT dispersion into films and phosphate crosslinking decreased water solubilities and surface wettability of films. The large deviation in data between different samples indicated the potential of films to be tailored depending on the specific application. Orange peel oil also preserved its antimicrobial activity inside GG films, depicted by visible inhibition zones on both Gr− and Gr+ bacterial cultures and was also able to slow down the spoilage of strawberries. All the methods applied also were successful in improving the films' barrier properties. Findings showed the possibility of improving the physical properties of GG films with the methods employed and the addition of active packaging properties such as antimicrobial protection with essential oil incorporation.

## Author statement

**Emrah Kirtil**: Conceptualization, Investigation, Writing - Original Draft, Writing - Review & Editing, Visualization.
**Ayca Aydogdu:** Conceptualization, Methodology, Investigation.
**Tatyana Svitova:** Investigation.
**Clayton Radke**: Supervision.

## Acknowledgments

Aydogdu A. has received financial support from The Scientific and Technological Research Council of Turkey (TUBITAK)-2214A Fellowship program. Kirtil E. has received financial support from Fulbright Turkey as part of the Ph.D. Dissertation Research Grant program.

## Appendix A. Supplementary data

Supplementary material related to this article can be found, in the online version, at doi:https://doi.org/10.1016/j.fpsl.2021.100687.

## References

Aboagye, D., Banadda, N., Kiggundu, N., & Kabenge, I. (2017). Assessment of orange peel waste availability in Ghana and potential bio-oil yield using fast pyrolysis. *Renewable and Sustainable Energy Reviews*. https://doi.org/10.1016/j.rser.2016.11.262

Acevedo-Fani, A., Salvia-Trujillo, L., Rojas-Graü, M. A., & Martín-Belloso, O. (2015). Edible films from essential-oil-loaded nanoemulsions: Physicochemical characterization and antimicrobial properties. *Food Hydrocolloids, 47*, 168–177. https://doi.org/10.1016/j.foodhyd.2015.01.032

Ahmadi, R., Kalbasi-Ashtari, A., Oromiehie, A., Yarmand, M.-S., & Jahandideh, F. (2012). Development and characterization of a novel biodegradable edible film obtained from psyllium seed (Plantago ovata Forsk). *Journal of Food Engineering, 109*(4), 745–751. https://doi.org/10.1016/j.jfoodeng.2011.11.010

Anal, A. K., Shrestha, S., & Sadiq, M. B. (2019). Biopolymeric-based emulsions and their effects during processing, digestibility and bioaccessibility of bioactive compounds in food systems. *Food Hydrocolloids, 87*(August (2018)), 691–702. https://doi.org/10.1016/j.foodhyd.2018.09.008

Aphibanthammakit, C., Nigen, M., Gaucel, S., Sanchez, C., & Chalier, P. (2018). Surface properties of Acacia senegal vs Acacia seyal films and impact on specific functionalities. *Food Hydrocolloids, 82*, 519–533. https://doi.org/10.1016/j.foodhyd.2018.04.032

Atef, M., Rezaei, M., & Behrooz, R. (2015). Characterization of physical, mechanical, and antibacterial properties of agar-cellulose bionanocomposite films incorporated with

savory essential oil. *Food Hydrocolloids*. https://doi.org/10.1016/j.foodhyd.2014.09.037
Aydogdu, A., Kirtil, E., Sumnu, G., Oztop, M. H., & Aydogdu, Y. (2018). Utilization of lentil flour as a biopolymer source for the development of edible films. *Journal of Applied Polymer Science*. https://doi.org/10.1002/app.46356
Azeredo, H. M. C., Rodrigues, T. H. S., Rodrigues, D. C., Cunha, A. P., Silva, L. M. A., & Gallão, M. I. (2017). Emulsion films from tamarind kernel xyloglucan and sesame seed oil by different emulsification techniques. *Food Hydrocolloids, 77*, 270–276. https://doi.org/10.1016/j.foodhyd.2017.10.003
Bahram, S., Rezaei, M., Soltani, M., Kamali, A., Ojagh, S. M., & Abdollahi, M. (2014). Whey protein concentrate edible film activated with cinnamon essential oil. *Journal of Food Processing and Preservation*. https://doi.org/10.1111/jfpp.12086
Benbettaïeb, N., Gay, J. P., Karbowiak, T., & Debeaufort, F. (2016). Tuning the functional properties of polysaccharide–Protein bio-based edible films by chemical, enzymatic, and physical cross-linking. *Comprehensive Reviews in Food Science and Food Safety, 15*(4), 739–752. https://doi.org/10.1111/1541-4337.12210
Bertuzzi, M. A., Castro Vidaurre, E. F., Armada, M., & Gottifredi, J. C. (2007). Water vapor permeability of edible starch based films. *Journal of Food Engineering, 80*(3), 972–978. https://doi.org/10.1016/j.jfoodeng.2006.07.016
Borges, A. M. G., Banegas, R. S., Porto, L. C., Zornio, C. F., & Soldi, V. (2013). Preparation, characterization and properties of films obtained from cross-linked guar gum. *Polímeros Ciência e Tecnologia, 23*(2), 182–188. https://doi.org/10.4322/polimeros.2013.082
Cano, A., Fortunati, E., Cháfer, M., Kenny, J. M., Chiralt, A., & González-Martínez, C. (2015). Properties and ageing behaviour of pea starch films as affected by blend with poly(vinyl alcohol). *Food Hydrocolloids, 48*, 84–93. https://doi.org/10.1016/j.foodhyd.2015.01.008
Casariego, A., Souza, B. W. S., Cerqueira, M. A., Teixeira, J. A., Cruz, L., Díaz, R., et al. (2009). Chitosan/clay films' properties as affected by biopolymer and clay micro/nanoparticles' concentrations. *Food Hydrocolloids*. https://doi.org/10.1016/j.foodhyd.2009.02.007
Chang, C., & Nickerson, M. T. (2015). Effect of protein and glycerol concentration on the mechanical, optical, and water vapor barrier properties of canola protein isolate-based edible films. *Food Science and Technology International, 21*(1), 33–44. https://doi.org/10.1177/1082013213503645
Costa, M. J., Marques, A. M., Pastrana, L. M., Teixeira, J. A., Sillankorva, S. M., & Cerqueira, M. A. (2018). Physicochemical properties of alginate-based films: Effect of ionic crosslinking and mannuronic and guluronic acid ratio. *Food Hydrocolloids, 81*, 442–448. https://doi.org/10.1016/j.foodhyd.2018.03.014
Dias, A. B., Müller, C. M. O., Larotonda, F. D. S., & Laurindo, J. B. (2010). Biodegradable films based on rice starch and rice flour. *Journal of Cereal Science, 51*(2), 213–219. https://doi.org/10.1016/j.jcs.2009.11.014
Dick, M., Costa, T. M. H., Gomaa, A., Subirade, M., Rios, A. D. O., & Flôres, S. H. (2015). Edible film production from chia seed mucilage: Effect of glycerol concentration on its physicochemical and mechanical properties. *Carbohydrate Polymers, 130*, 198–205. https://doi.org/10.1016/j.carbpol.2015.05.040
Fan, H. Y., Duquette, D., Dumont, M. J., & Simpson, B. K. (2018). Salmon skin gelatin-corn zein composite films produced via crosslinking with glutaraldehyde: Optimization using response surface methodology and characterization. *International Journal of Biological Macromolecules, 120*, 263–273. https://doi.org/10.1016/j.ijbiomac.2018.08.084
Fennema, O. R. (1996). *Food chemistry* (third edition). Marcel Dekker, Inc.. https://doi.org/10.1016/0260-8774(88)90055-6
Fernández, L., De Apodaca, E. D., Cebrián, M., Villarán, M. C., & Maté, J. I. (2007). Effect of the unsaturation degree and concentration of fatty acids on the properties of WPI-based edible films. *European Food Research and Technology*. https://doi.org/10.1007/s00217-006-0305-1
Galus, S. (2018). Functional properties of soy protein isolate edible films as affected by rapeseed oil concentration. *Food Hydrocolloids, 85*(July), 233–241. https://doi.org/10.1016/j.foodhyd.2018.07.026
Galus, S., & Kadzińska, J. (2016). Whey protein edible films modified with almond and walnut oils. *Food Hydrocolloids*. https://doi.org/10.1016/j.foodhyd.2015.06.013
Gliko-Kabir, I., Penhasi, A., & Rubinstein, A. (1999). Characterization of crosslinked guar by thermal analysis. *Carbohydrate Research, 316*(1–4), 6–13. https://doi.org/10.1016/S0008-6215(99)00025-7
Gliko-Kabir, I., Yagen, B., Penhasi, A., & Rubinstein, A. (2000). Phosphated crosslinked guar for colon-specific drug delivery - I. Preparation and physicochemical characterization. *Journal of Controlled Release, 63*(1–2), 121–127. https://doi.org/10.1016/S0168-3659(99)00179-0
Gomaa, M., Hifney, A. F., Fawzy, M. A., & Abdel-gawad, K. M. (2018). Use of seaweed and filamentous fungus derived polysaccharides in the development of alginate-chitosan edible films containing fucoidan: Study of moisture sorption, polyphenol release and antioxidant properties. *Food Hydrocolloids, 82*, 239–247. https://doi.org/10.1016/j.foodhyd.2018.03.056
Gontard, N., Guilbert, S., & Cuq, J.-L. (1992). Edible wheat gluten films: Influence of the main process variables on film properties using response surface methodology. *Journal of Food Science, 57*(1), 190–195. https://doi.org/10.1111/j.1365-2621.1992.tb05453.x
Guerreiro, T. M., de Oliveira, D. N., Melo, C. F. O. R., de Oliveira Lima, E., & Catharino, R. R. (2018). Migration from plastic packaging into meat. *Food Research International, 109*(April), 320–324. https://doi.org/10.1016/j.foodres.2018.04.026
Gutiérrez, T. J., Guzmán, R., Medina Jaramillo, C., & Famá, L. (2016). Effect of beet flour on films made from biological macromolecules: Native and modified plantain flour. *International Journal of Biological Macromolecules, 82*, 395–403. https://doi.org/10.1016/j.ijbiomac.2015.10.020
Gutiérrez, T. J., Morales, N. J., Pérez, E., Tapia, M. S., & Famá, L. (2015). Physico-chemical properties of edible films derived from native and phosphated cush-cush yam and cassava starches. *Food Packaging and Shelf Life, 3*, 1–8. https://doi.org/10.1016/j.fpsl.2014.09.002
Hernandez, R. J. (1994). Effect of water vapor on the transport properties of oxygen through polyamide packaging materials. *Journal of Food Engineering*. https://doi.org/10.1016/0260-8774(94)90050-7
Hoque, M. S., Benjakul, S., & Prodpran, T. (2010). Effect of heat treatment of film-forming solution on the properties of film from cuttlefish (Sepia pharaonis) skin gelatin. *Journal of Food Engineering*. https://doi.org/10.1016/j.jfoodeng.2009.06.046
Huang, T., Tu, Z., Shangguan, X., Sha, X., Wang, H., Zhang, L., et al. (2019). Fish gelatin modifications: A comprehensive review. *Trends in Food Science & Technology, 86*(February), 260–269. https://doi.org/10.1016/j.tifs.2019.02.048
Hussain, F., Chen, J., & Hojjati, M. (2007). Epoxy-silicate nanocomposites: Cure monitoring and characterization. *Materials Science and Engineering A*. https://doi.org/10.1016/j.msea.2006.09.071
Kang, H. J., & Min, S. C. (2010). Potato peel-based biopolymer film development using high-pressure homogenization, irradiation, and ultrasound. *LWT - Food Science and Technology*. https://doi.org/10.1016/j.lwt.2010.01.025
Ke, J., Xiao, L., Yu, G., Wu, H., Shen, G., & Zhang, Z. (2019). The study of diffusion kinetics of cinnamaldehyde from corn starch-based film into food simulant and physical properties of antibacterial polymer film. *International Journal of Biological Macromolecules, 125*, 642–650. https://doi.org/10.1016/j.ijbiomac.2018.12.094
Kotsampasi, B., Tsiplakou, E., Christodoulou, C., Mavrommatis, A., Mitsiopoulou, C., Karaiskou, C., et al. (2018). Effects of dietary orange peel essential oil supplementation on milk yield and composition, and blood and milk antioxidant status of dairy ewes. *Animal Feed Science and Technology*. https://doi.org/10.1016/j.anifeedsci.2018.08.007
Kowalczyk, D., Gustaw, W., Zieba, E., Lisiecki, S., Stadnik, J., & Baraniak, B. (2016). Microstructure and functional properties of sorbitol-plasticized pea protein isolate emulsion films: Effect of lipid type and concentration. *Food Hydrocolloids, 60*, 353–363. https://doi.org/10.1016/j.foodhyd.2016.04.006
Lee, M. H., Kim, S. Y., & Park, H. J. (2018). Effect of halloysite nanoclay on the physical, mechanical, and antioxidant properties of chitosan films incorporated with clove essential oil. *Food Hydrocolloids, 84*(May), 58–67. https://doi.org/10.1016/j.foodhyd.2018.05.048
Lei, Y., Wu, H., Jiao, C., Jiang, Y., Liu, R., Xiao, D., et al. (2019). Investigation of the structural and physical properties, antioxidant and antimicrobial activity of pectin-konjac glucomannan composite edible films incorporated with tea polyphenol. *Food Hydrocolloids, 94*(December 2018), 128–135. https://doi.org/10.1016/j.foodhyd.2019.03.011
Lequeu, J., Fauconnier, M. L., Chammaï, A., Bronner, R., & Blée, E. (2003). Formation of plant cuticle: Evidence for the occurrence of the peroxygenase pathway. *The Plant Journal*. https://doi.org/10.1046/j.1365-313X.2003.01865.x
Li, K., Zhu, J., Guan, G., & Wu, H. (2019). Preparation of chitosan-sodium alginate films through layer-by-layer assembly and ferulic acid crosslinking: Film properties, characterization, and formation mechanism. *International Journal of Biological Macromolecules, 122*, 485–492. https://doi.org/10.1016/j.ijbiomac.2018.10.188
Liu, J., Wang, H., Wang, P., Guo, M., Jiang, S., Li, X., et al. (2018). Films based on κ-carrageenan incorporated with curcumin for freshness monitoring. *Food Hydrocolloids, 83*, 134–142. https://doi.org/10.1016/j.foodhyd.2018.05.012
Liu, Q. R., Wang, W., Qi, J., Huang, Q., & Xiao, J. (2019). Oregano essential oil loaded soybean polysaccharide films: Effect of Pickering type immobilization on physical and antimicrobial properties. *Food Hydrocolloids, 87*(August 2018), 165–172. https://doi.org/10.1016/j.foodhyd.2018.08.011
Ma, Q., Zhang, Y., Critzer, F., Davidson, P. M., Zivanovic, S., & Zhong, Q. (2015). Physical, mechanical, and antimicrobial properties of chitosan films with microemulsions of cinnamon bark oil and soybean oil. *Food Hydrocolloids*. https://doi.org/10.1016/j.foodhyd.2015.07.036
Mali, S., Grossmann, M. V. E., Garcia, M. A., Martino, M. N., & Zaritzky, N. E. (2004). Barrier, mechanical and optical properties of plasticized yam starch films. *Carbohydrate Polymers, 56*(2), 129–135. https://doi.org/10.1016/j.carbpol.2004.01.004
McHugh, T. H., Avenabustillos, R., & Krochta, J. M. (1993). Hydrophilic edible films - modified procedure for water-vapor permeability and explanation of thickness effects. *Journal of Food Science, 58*(4), 899–903. https://doi.org/10.1111/j.1365-2621.1993.tb09387.x
Meira, S. M. M., Zehetmeyer, G., Werner, J. O., & Brandelli, A. (2017). A novel active packaging material based on starch-halloysite nanocomposites incorporating antimicrobial peptides. *Food Hydrocolloids, 63*, 561–570. https://doi.org/10.1016/j.foodhyd.2016.10.013
Moreira, R., Chenlo, F., Silva, C., Torres, M. D., Díaz-Varela, D., Hilliou, L., et al. (2012). Surface tension and refractive index of guar and tragacanth gums aqueous dispersions at different polymer concentrations, polymer ratios and temperatures. *Food Hydrocolloids, 28*(2), 284–290. https://doi.org/10.1016/j.foodhyd.2012.01.007
Musso, Y. S., Salgado, P. R., & Mauri, A. N. (2017). Smart edible films based on gelatin and curcumin. *Food Hydrocolloids, 66*, 8–15. https://doi.org/10.1016/j.foodhyd.2016.11.007
Nascimento, T. A., Calado, V., & Carvalho, C. W. P. (2012). Development and characterization of flexible film based on starch and passion fruit mesocarp flour with nanoparticles. *Food Research International*. https://doi.org/10.1016/j.foodres.2012.07.051
Ojagh, S. M., Rezaei, M., Razavi, S. H., & Hosseini, S. M. H. (2010). Development and evaluation of a novel biodegradable film made from chitosan and cinnamon essential

oil with low affinity toward water. *Food Chemistry*. https://doi.org/10.1016/j.foodchem.2010.02.033

Pelissari, F. M., Andrade-Mahecha, M. M., Sobral, P. J. A., & Menegalli, F. C. (2013a). Comparative study on the properties of flour and starch films of plantain bananas (Musa paradisiaca). *Food Hydrocolloids, 30*(2), 681–690. https://doi.org/10.1016/j.foodhyd.2012.08.007

Pelissari, F. M., Andrade-Mahecha, M. M., Sobral, P. J. A., & Menegalli, F. C. (2013b). Optimization of process conditions for the production of films based on the flour from plantain bananas (Musa paradisiaca). *LWT - Food Science and Technology, 52*(1), 1–11. https://doi.org/10.1016/j.lwt.2013.01.011

Pereda, M., Amica, G., & Marcovich, N. E. (2012). Development and characterization of edible chitosan/olive oil emulsion films. *Carbohydrate Polymers*. https://doi.org/10.1016/j.carbpol.2011.09.019

Ragaert, P., Verbeke, W., Devlieghere, F., & Debevere, J. (2004). Consumer perception and choice of minimally processed vegetables and packaged fruits. *Food Quality and Preference*. https://doi.org/10.1016/S0950-3293(03)00066-1

Rocha Plácido Moore, G., Maria Martelli, S., Gandolfo, C., José do Amaral Sobral, P., & Borges Laurindo, J. (2006). Influence of the glycerol concentration on some physical properties of feather keratin films. *Food Hydrocolloids, 20*(7), 975–982. https://doi.org/10.1016/j.foodhyd.2005.11.001

Rutkevičius, M., Allred, S., Velev, O. D., & Velikov, K. P. (2018). Stabilization of oil continuous emulsions with colloidal particles from water-insoluble plant proteins. *Food Hydrocolloids, 82*, 89–95. https://doi.org/10.1016/j.foodhyd.2018.04.004

Sgorla, D., Almeida, A., Azevedo, C., Bunhak, É. J., Sarmento, B., & Cavalcanti, O. A. (2016). Development and characterization of crosslinked hyaluronic acid polymeric films for use in coating processes. *International Journal of Pharmaceutics, 511*(1), 380–389. https://doi.org/10.1016/j.ijpharm.2016.07.033

Singh, T. P., Chatli, M. K., & Sahoo, J. (2015). Development of chitosan based edible films: Process optimization using response surface methodology. *Journal of Food Science and Technology, 52*(5), 2530–2543. https://doi.org/10.1007/s13197-014-1318-6

Svitova, T., Leung, T., & Lin, M. C. (2010). Dynamics of contact lens-surface wettability in vitro: Effect of dehydration-rehydration cycles. *Investigative Ophthalmology & Visual Science, 51*(13), 3427.

Tajeddin, B., Rahman, R. A., & Abdulah, L. C. (2010). The effect of polyethylene glycol on the characteristics of kenaf cellulose/low-density polyethylene biocomposites. *International Journal of Biological Macromolecules*. https://doi.org/10.1016/j.ijbiomac.2010.04.004

Variyar, P. S., Bahadur, J., Gupta, S., Sharma, A., Mazumder, S., & Saurabh, C. K. (2015). Mechanical and barrier properties of guar gum based nano-composite films. *Carbohydrate Polymers, 124*, 77–84. https://doi.org/10.1016/j.carbpol.2015.02.004

Verma, D., & Sharma, S. K. (2021). Recent advances in guar gum based drug delivery systems and their administrative routes. *International Journal of Biological Macromolecules* (Vol. 181,, 653–671. https://doi.org/10.1016/j.ijbiomac.2021.03.087. Elsevier B.V.

Wang, Z., Zhou, J., Wang, X., Zhang, N., Sun, X., & Ma, Z. (2014). The effects of ultrasonic/microwave assisted treatment on the water vapor barrier properties of soybean protein isolate-based oleic acid/stearic acid blend edible films. *Food Hydrocolloids*. https://doi.org/10.1016/j.foodhyd.2013.07.006

Wu, H., Lei, Y., Zhu, R., Zhao, M., Lu, J., Xiao, D., et al. (2019). Preparation and characterization of bioactive edible packaging films based on pomelo peel flours incorporating tea polyphenol. *Food Hydrocolloids, 90*(December 2018), 41–49. https://doi.org/10.1016/j.foodhyd.2018.12.016

Xiao, L., Wang, B., Yang, G., & Gauthier, M. (2012). Poly(Lactic acid)-Based biomaterials: Synthesis, modification and applications. *Biomedical Science, Engineering and Technology*. https://doi.org/10.5772/23927

Yıldırım-Yalçın, M., Şeker, M., & Sadıkoğlu, H. (2019). Development and characterization of edible films based on modified corn starch and grape juice. *Food Chemistry, 292*, 6–13. https://doi.org/10.1016/j.foodchem.2019.04.006

Yin, S.-W., Zhao, Z.-G., Yin, Y., Yang, X.-Q., Shi, W.-J., Tang, C.-H., et al. (2015). Development and characterization of novel chitosan emulsion films via pickering emulsions incorporation approach. *Food Hydrocolloids, 52*, 253–264. https://doi.org/10.1016/j.foodhyd.2015.07.008

Zúñiga, R. N., Skurtys, O., Osorio, F., Aguilera, J. M., & Pedreschi, F. (2012). Physical properties of emulsion-based hydroxypropyl methylcellulose films: Effect of their microstructure. *Carbohydrate Polymers*. https://doi.org/10.1016/j.carbpol.2012.06.066